Ionic Liquids

DOI: 10.1002/anie.201004955

The Importance of Hydrogen Bonds for the Structure of Ionic Liquids: Single-Crystal X-ray Diffraction and Transmission and Attenuated Total Reflection Spectroscopy in the Terahertz Region**

Christian Roth, Tim Peppel, Koichi Fumino, Martin Köckerling, and Ralf Ludwig**

The importance of hydrogen bonding in imidazolium-based ionic liquids (ILs) is the subject of highly controversial discussions.[1–23] Because ILs solely exist of anions and cations, it is generally assumed that Coulomb interactions absolutely dominate the properties of these materials. However, determining hydrogen-bonding environments is critical for the understanding of the modes of interaction and conformational influences of IL cations and anions on the lattice energies, melting points, and general behavior of ILs. Recently, we reported the enhanced cation–anion interaction that is due to hydrogen bonding in pure imidazolium-based ionic liquids by far-infrared spectroscopy.[24] The observed frequency shifts could be related to increased force constants indicating stronger cation–anion interactions. Ab initio methods suggested a close relationship between the calculated interaction energies of IL aggregates and the measured intermolecular stretching frequencies.[24] Both properties are related to increasing H-bond capabilities in the different imidazolium cations. This finding clearly indicates that the stretching frequencies are a direct measure for hydrogen bonding in the ILs. However, an ultimate test for the presence of H-bonding could be given by investigating imidazolium ionic liquids with no H-bond abilities, such as the alkylimidazolium NTf_2 salt with all the ring hydrogen atoms substituted by methyl groups, namely 1,2,3,4,5-pentamethylimidazolium bis(trifluoromethylsulfonyl)imide, (1,2,3,4,5-MIm)NTf_2 (**I**; Figure 1). The low vibrational frequencies and the structure of **I** should be significantly different from those for ILs containing substantial H-bond contributions. To test this prediction is very challenging. The commercially unavailable salt **I** is a solid at room temperature.[25] It melts at about 118 °C and is thus by definition not an ionic liquid. The low-frequency region between 10 and 100 cm^{-1} for the solid material is only accessible by a few methods, such as Raman spectroscopy, inelastic neutron scattering, far-infrared (FIR) or tetrahertz (THz) transmission spectroscopy, or attenuated total reflection (ATR) techniques.

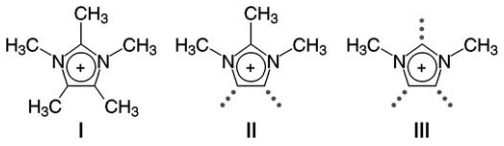

Figure 1. The cations of the imidazolium-based salts **I**–**III**. The position of possible H-bonds are indicated by the dotted lines.

Herein we synthesized compound **I**, determined its single-crystal X-ray structure, and measured the transmission FIR and THz as well as THz ATR spectra on this salt. The vibrational bands of the measured spectra between 10 and 100 cm^{-1} could be fully assigned to specific intermolecular interactions, although unspecific collective vibrational modes are usually expected in this low-frequency range. Moreover we could confirm our prediction that pure ionic interactions give low-frequency vibrational bands, which shift to higher wavenumbers with increasing H-bond abilities and H-bond strength. Overall, this study demonstrates the power of FIR and THz spectroscopy for recognizing and classifying interactions between cations and anions in liquid and solid-state materials.

Compound **I** was prepared by metathesis of 1,2,3,4,5-pentamethylimidazolium iodide with Li(NTf_2). DSC analysis showed a sharp melting transition at 118 °C consistent with the literature.[10,25]

The infrared spectra of **I** were measured using a high-pressure mercury lamp, giving spectra down to 10 cm^{-1}. Polyethylene (PE) pellets of 4 mm thickness gave no fringe artifacts from internal reflections within the pellets. The resulting spectra, presented in Figure 2, show three broad vibrational bands within the frequency range 10 to 100 cm^{-1} (0.3–3.0 THz). Repeating the pellet measurement with THz pulsed spectroscopy gives a similar spectrum. Both transmission spectra can be joined together smoothly. However, measurements in a polyethylene (PE) matrix involve mixing and compressing, which could induce a polymorphic change in the sample, as is known for molecular compounds. The ATR technique thus simplifies the collection of spectra owing

[*] C. Roth, Dr. K. Fumino, Prof. Dr. R. Ludwig
Universität Rostock, Institut für Chemie
Abteilung für Physikalische Chemie
Dr. Lorenz Weg 1, 18059 Rostock (Germany)
Fax: (+49) 381-498-6517
E-mail: ralf.ludwig@uni-rostock.de
T. Peppel, Prof. Dr. M. Köckerling
Universität Rostock, Institut für Chemie
Abteilung für Anorganische Chemie
Albert-Einstein-Strasse 3a, 18059 Rostock (Germany)
Fax: (+49) 381-498-6390
E-mail: martin.koeckerling@uni-rostock.de
Prof. Dr. R. Ludwig
Leibniz-Institut für Katalyse an der Universität Rostock e.V.
Albert-Einstein-Strasse 29a, 18059 Rostock (Germany)

[**] This work was supported by the DFG priority programme SPP 1191 "Ionic Liquids" and by the Sonderforschungsbereich SFB 652.

Supporting information for this article is available on the WWW under http://dx.doi.org/10.1002/anie.201004955.

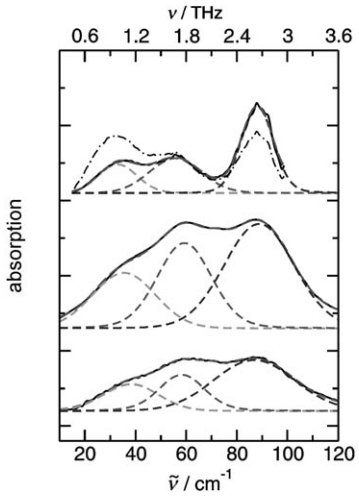

Figure 2. Spectra of compound **I** in the THz region: FIR transmission spectrum (bottom), THz transmission spectrum (middle) and THz ATR spectrum (top). The observed THz ATR spectrum (dot–dash line) has been corrected for the wavenumber-dependent variation in penetration depth (red curve). The dotted lines indicate the three dominant contributions obtained from the deconvolution of all of the measured spectra. The FIR and THz transmission spectra show the same shape but different intensities, because varying sample amounts had to be used in both experiments.

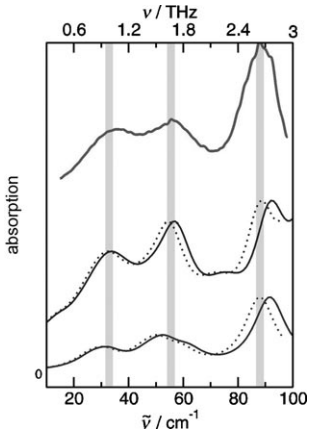

Figure 3. The deconvoluted THz ATR spectrum (top) of **I** compared to DFT calculated spectra for the monomer (bottom) and trimer of ion-pair aggregates. The calculated spectra corrected for the harmonic approximation are given by the dotted lines. The three dominant vibrational bands are observed in all of the spectra.

to the ease and speed of sampling. This technique uses a small sampling area, requires no special sample preparation, and is non-destructive. Therefore we applied the terahertz ATR technique to measure the low-frequency spectra of **I** between 10 and 100 cm^{-1}. The measured ATR spectrum is shown in Figure 2 along with the FIR and THz transmission spectra. As there is a wavenumber-dependent variation in penetration depth, the ATR signal must be corrected to approximately the correct absorption (see Supporting Information). However, it has been shown that this correction does not lead to significant frequency shifts in this frequency range.[26] In principle, the ATR THz spectrum shows the same but more distinct features as the FIR and THz transmission spectra using the PE pellets.

The assignment of the low frequency vibrational bands will be supported by DFT calculation on monomers and trimers of ion airs of **I**. The frequencies were calculated and given as Lorentzian curves with a half width of about 7 cm^{-1}. Figure 3 shows a nearly perfect agreement between the measured and the calculated spectra for all cluster species, which is somewhat surprising because our calculations do not take crystal packing effects into account. In recent THz solid-state measurements of ecstasy, Allis et al. underlined the significance of these effects but also stated that calculations of isolated-molecule normal modes is an important step in support of the solid-state normal analysis.[27] However, in our study there are neither cooperative effects nor specific local interactions with increasing cluster size.

The DFT calculated frequencies now allow an assignment of the vibrational modes, which are usually summarized as lattice motions. For that purpose all the measured FIR and THz spectra were deconvoluted into three distinct vibrational contributions. The vibrational bands at about 90 cm^{-1} can be clearly assigned to hindered rotations of the imidazolium methyl groups. These contributions stemming from the five methyl groups in **I** are particularly strong in the solid material. The lowest frequencies at about 35 cm^{-1} will be assigned to sharing motions of cations and anions in the IL. The most-desirable stretching anion–cation interaction can be referred to the vibrational band found between 55 and 59 cm^{-1}.

All frequencies for the anion–cation interaction are listed in Table 1. The transmission and ATR frequencies in the solid phase are given for the ILs **I** and **II**; literature data are added for the ILs **II** and **III** as observed in the liquid phase.[24] Liquid- and solid-phase spectra are only available for the IL **II**. The solid-phase frequencies are shifted to higher wavenumbers, which is probably caused by a stronger interaction. Taking this shift into account, the solid-phase frequencies for **I** ranging between 55 and 59 cm^{-1} fit well into the relationship between the calculated binding energies and the vibrational bands as obtained for the liquid phase (Figure 4). Obviously, the shift to higher wavenumbers can be related to an enhanced anion–cation interaction due to hydrogen bonding in these ILs. Because of missing H-bonding in **I**, the vibrational band is weak in intensity and low in frequency. In IL **III**, H-bond formation is possible with C2-H, C4-H, and C5-H. By subtracting the binding energies in **I** (where no H-bonds are present) from those in **III**, we can estimate the H-bond

Table 1: Low vibrational frequencies [cm^{-1}] describing the anion–cation interactions in **I–III** measured by FIR and THz spectroscopy.

IL	FIR[24] transmission liquid	FIR transmission solid (pellet)	THz transmission solid (pellet)	THz ATR solid
I	–	58.3	59.3	55.5
II	59.3	66.3	68.6	62.3
III	85.7	–	–	–

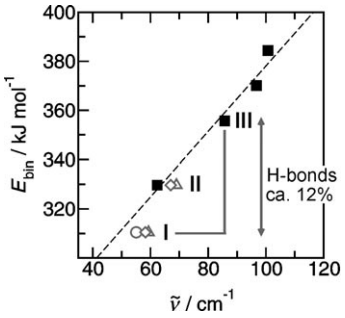

Figure 4. Average interaction energies E_{bin} per ion pair in tetramers of the ILs (1,2,3-MIm)NTf_2 (**II**), (1,3-MIm)NTf_2, (1,2-MIm)NTf_2, and (1-MIm)NTf_2 in the liquid phase plotted versus the measured frequencies $\nu(^+C\cdots A^-)$ from literature (■, from left to right)[24] For the ILs (1,2,3,4,5-MIm)NTf_2 (**I**) and **II** the FIR transmission (◇); THz transmission (△); THz ATR (○) frequencies are given.

contribution to be 40 kJ mol^{-1} and thus only 12% of the overall interaction energy (see Figure 4). Although this value is a result of some approximations, the magnitude of H-bonding is reasonable, as shown in other studies.[28] We have thus shown that hydrogen bonding is of significant importance and that the even small local interactions lead to characteristically different X-ray structures for the ILs **I** and **III**.

The existence of H-bonding in imidazolium ionic liquids is also supported by comparing the X-ray structure of **I**[29] with that of 1,3-dimethylimidazolium bis(trifluoromethylsulfonyl)imide (1,3-MIm)NTf_2, **III**) reported by Holbrey et al.[6] In **III** the NTf_2^- anion is hydrogen-bonded to three equatorially arrayed 1,3-dimethylimidazolium cations (with C2-H, C4-H, and C5-H) through C–H···O and C–H···N contacts between the cations and the anions with an additional imidazolium cation below each anion, from the next layer of the double layer. Holbrey et al. reported seven hydrogen bonding interactions from hydrogen atoms of the cations to either oxygen or nitrogen atoms of the anions. Surprisingly, they found an unusual higher energy conformation with the two S–CF_3 groups *cis* to each other. Holbrey et al. assumed that this behavior is caused by structural constraints of extensive C–H···O cation–anion hydrogen-bonding in the lattice.[6]

Because of missing H-bonds, the structure of **I** is completely different. Figure 5 shows the molecular structure

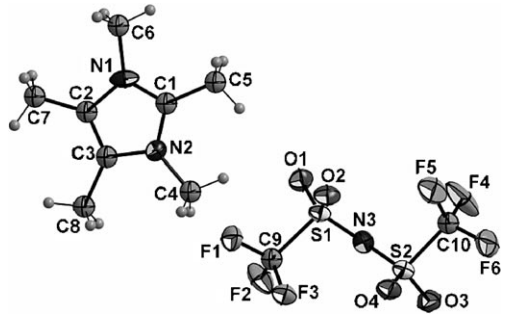

Figure 5. View of the molecular structure of **I** (thermal ellipsoids are set at 50% probability). The isolated ions show no specific interactions resulting in the *trans* conformation of the anion, which is the lowest in energy.

obtained by single-crystal X-ray diffraction. Even though all the flat cations are arranged parallel to each other (see Figure 6), no hydrogen-bonded sheets are formed (no stacking) and only the *trans* conformation for the anion is found. There are no constraints by H-bonding for structure formation and the lower energy conformation is adapted.

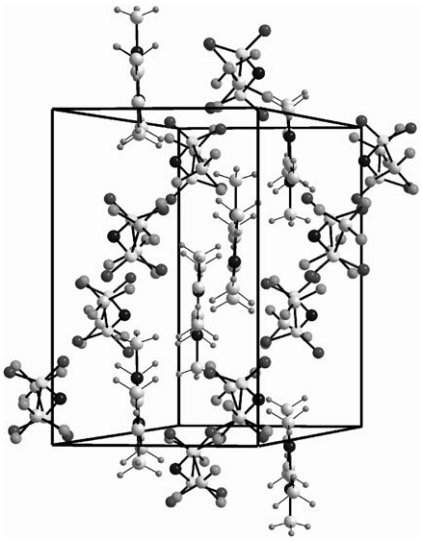

Figure 6. View of the unit cell contents of **I**, showing the parallel arrangement without stacking of the flat cations.

With a combined FIR, THz, single-crystal X-ray diffraction and DFT studies, we could demonstrate that H-bonds exist in imidazolium-based ionic liquids. Although this local and directional type of interaction contributes only one tenth of the overall interaction energy, H-bonds have significant influence on the structure of these Coulomb systems. With increasing H-bond abilities and strengths, the NTf_2^- anion is found in the *cis* configuration. Switching off these local interactions leads to the energetically favored *trans* conformation. These structural effects caused by hydrogen bonding should have significant influence on IL properties, such as melting points and viscosities. This work is currently ongoing in our laboratories.

Experimental Section

Compound **I** was synthesized in 70% yield by a metathesis reaction of 1,2,3,4,5-pentamethylimidazolium iodide (prepared according to Refs [25,30]) with Li(NTf_2). Compounds **II** and **III** were purchased from Iolitec GmbH (Denzlingen, Germany). For the only room-temperature IL (**III**), the water content was found to be 56 ppm, as determined by Karl Fischer titration. IL **II** is solid at room temperature and was used as delivered.

The FTIR measurements were performed with a Bruker Vertex 70 FTIR spectrometer equipped with an extension for measurements in the FIR region that consists a multilayer mylar beam splitter, a room-temperature DLATGS detector with preamplifier, and polyethylene windows for the internal optical path. The accessible spectral region for this configuration lies between 30 and 680 cm^{-1} (0.3 and 20.3 THz). Further improvement could be achieved by using a high-pressure mercury lamp and an silica beam splitter. This configuration allows measurements down to 10 cm^{-1} and significantly better signal-

to-noise ratios. The solid ILs were mixed with polyethylene powder and measured as pellets in the FIR region.

The THz spectroscopy measurements were made using a Tera-View TPS spectra 3000 spectrometer. For all of the measurements, the sample compartment of the spectrometer was purged with dry nitrogen at 10 litres per minute. The transmission terahertz spectra of the PE/IL pellets were collected from 2 cm^{-1} to 120 cm^{-1} at a resolution of 1.2 cm^{-1}. Each rapid-scan spectrum, which is the average of 18000 co-added scans, took 60 s to record.

The pulsed terahertz attenuated total reflection (ATR) spectra were recorded with the same THz pulsed spectrometer and a silicon ATR module. The silicon ATR crystal is cut at angle of 45°. These THz ATR spectra could be recorded from 15 to 100 cm^{-1} (0.2 to 3 THz) at a resolution of 1.2 cm^{-1}.

The frequencies for monomers and trimers of ion pairs of **I** were calculated at the B3LYP-6-31 + G* level of theory using the Gaussian 03 program.[32] The larger tetramers for all ILs (including four ion pairs) could be calculated only at the Hartree–Fock level using the internal stored 3-21G basis set.[32] The binding energies and average binding energies per ion were been corrected for the basis set superposition error (BSSE).[33]

Further details of the experimental procedures are given in the Supporting Information.

Received: August 9, 2010
Revised: August 31, 2010
Published online: December 3, 2010

Keywords: density functional calculations · hydrogen bonds · ionic liquids · terahertz spectroscopy · X-ray diffraction

[1] *Ionic Liquids in Synthesis*, 2nd ed. (Ed.: P. Wasserscheid, T. Welton), Wiley-VCH, Weinheim, **2007**.
[2] H. Weingärtner, *Angew. Chem.* **2008**, *120*, 664 – 682; *Angew. Chem. Int. Ed.* **2008**, *47*, 654 – 670.
[3] A. K. Abdul-Sada, A. M. Greenway, P. B. Hitchcock, T. J. Mohammed, K. R. Seddon, J. A Zora, *J. Chem. Soc. Chem. Commun.* **1986**, 1753 – 1754.
[4] P. B. Hitchcock, K. R. Seddon, T. J. Welton, *J. Chem. Soc. Dalton Trans.* **1993**, 2639 – 2643.
[5] J. D. Holbrey, W. M. Reichert, M. Nieuwenhuyzen, S. Johnston, K. R. Seddon, R. D. Rogers, *Chem. Commun.* **2003**, 1636 – 1637.
[6] J. D. Holbrey, W. M. Reichert, R. D. Rogers, *Dalton Trans.* **2004**, 2267 – 2271.
[7] J. D. Holbrey, W. M. Reichert, M. Nieuwenhuyzen, O. Sheppard, C. Hardacre, R. D. Rogers, *Chem. Commun.* **2004**, 2267 – 2271.
[8] P. Bonhôte, A.-P. Dias, N. Papageorgiou, K. Kalynasundaram, M. Grätzel, *Inorg. Chem.* **1996**, *35*, 1168 – 1178.
[9] J. D. Tubbs, M. M. Hoffmann, *J. Solution Chem.* **2004**, *33*, 381 – 394.
[10] R. W. Berg, M. Deetlefs, K. R. Seddon, I. Shim, J. M. Thompson, *J. Phys. Chem. B* **2005**, *109*, 19018 – 19025.
[11] S. Katsyuba, E. E. Zvereva, A. Vidiš, Paul J. Dyson, *J. Phys. Chem. B* **2007**, *111*, 352 – 370.
[12] P. Hunt, *J. Phys. Chem. B* **2007**, *111*, 4844 – 4853.
[13] P. A. Hunt, B. Kirchner, T. Welton, *Chem. Eur. J.* **2006**, *12*, 6762 – 6775.
[14] S. Kossmann, J. Thar, B. Kirchner, P. A. Hunt, T. Welton, *J. Chem. Phys.* **2006**, *124*, 174506.
[15] B. L. Bhargava, S. J. Balasubramanian, *J. Chem. Phys.* **2007**, *127*, 114510.
[16] F. Dommert, J. Schmidt, B. Qiao, Y. Zhao, C. Krekeler, L. Delle Site, R. Berger, C. Holm, *J. Chem. Phys.* **2008**, *129*, 224501.
[17] J.-C. Lassègues, J. Gronding, D. Cavagnat, P. Johansson, *J. Phys. Chem. A* **2009**, *113*, 6419 – 6421.
[18] S. Tsuzuki, H. Tokuda, M. Mikami, *Phys. Chem. Chem. Phys.* **2007**, *9*, 4780 – 4784.
[19] Y. Jeon, J. Sung, C. Seo, H. Lim, H. Cheong, M. Kang, B. Ouchi, D. Kim, *J. Phys. Chem. B* **2008**, *112*, 4735 – 4740.
[20] A. Dominguez-Vidal, N. Kaun, M. Ayora-Cañada, B. Lendl, *J. Phys. Chem. B* **2007**, *111*, 4446 – 4452.
[21] K. Fumino, A. Wulf, R. Ludwig, *Angew. Chem.* **2008**, *120*, 3890 – 3894; *Angew. Chem. Int. Ed.* **2008**, *47*, 3830 – 3834.
[22] K. Fumino, A. Wulf, R. Ludwig, *Angew. Chem.* **2008**, *120*, 8859 – 8862; *Angew. Chem. Int. Ed.* **2008**, *47*, 8731 – 8734.
[23] T. Köddermann, K. Fumino, R. Ludwig, J. N. C. Lopes, A. A. H. Pádua, *ChemPhysChem* **2009**, *10*, 1181 – 1186.
[24] K. Fumino, A. Wulf, R. Ludwig, *Angew. Chem.* **2010**, *122*, 459 – 463; *Angew. Chem. Int. Ed.* **2010**, *49*, 449 – 453.
[25] H. L. Ngo, K. LeCompte, L. Hargens, A. B. McEwen, *Thermochim. Acta* **2000**, *357–358*, 97 – 102.
[26] Y. Ogawa, L. Cheng, S. Hayashi, K. Fukunaga, *IEICE Electron. Express* **2009**, *6*, 117 – 121.
[27] D. G. Allis, P. M. Hakey, T. M. Korter, *Chem. Phys. Lett.* **2008**, *463*, 353 – 356.
[28] K. Fumino, A. Wulf, R. Ludwig, *Phys. Chem. Chem. Phys.* **2009**, *11*, 8790 – 8794.
[29] Crystal structure analyses: X-ray diffraction data were collected using a Bruker-Nonius APEX-X8-CCD diffractometer with graphite-monochromated $Mo_{K\alpha}$ radiation ($\lambda = 0.71073$ Å). The structures were solved using the SHELXS-97 program (direct methods) and refined using SHELXL-97 (full-matrix least-squares refinements on F^2 data).[31] All H atoms were fixed on idealized positions and refined using riding models. **I**: colorless crystals, monoclinic, $P2_1/c$, (No. 14), $a = 18.3642(9)$, $b = 13.660(2)$, $c = 15.139(2)$ Å, $V = 1684.0(3)$ Å^3, $Z = 4$, $R1 = 0.0470$ ($I > 2\sigma(I)$), $wR2 = 0.1304$ (all data), 4302 symmetry-independent data, 226 parameters. CCDC 783124 contains the supplementary crystallographic data for this paper. These data can be obtained free of charge from The Cambridge Crystallographic Data Centre via www.ccdc.cam.ac.uk/data_request/cif.
[30] N. Kuhn, G. Henkel, J. Kreutzberg, *Z. Naturforsch. B* **1991**, *46*, 1706 – 1712.
[31] G. M. Sheldrick, *Acta Crystallogr. Sect. A* **2008**, *64*, 112 – 122.
[32] Gaussian 03 (Revision C.02), M. J. Frisch et al.; see the Supporting Information.
[33] S. Boys, F. Bernardi, *Mol. Phys.* **1970**, *19*, 553 – 566.

